More about Zener drag studies with Monte Carlo simulations

2013 Modelling Simul. Mater. Sci. Eng. 21 025007

(http://iopscience.iop.org/0965-0393/21/2/025007)

Modelling Simul. Mater. Sci. Eng. **21** (2013) 025007 (8pp) doi:10.1088/0965-0393/21/2/025007

More about Zener drag studies with Monte Carlo simulations

Carlos L Di Prinzio[1], Esteban Druetta[2] and Olga Beatriz Nasello[1]

[1] CONICET (Consejo Nacional de Ciencia y Tecnología) and Facultad de Matemática Astronomía y Física. Universidad Nacional de Córdoba, Medina Allende y Haya de la Torre, Ciudad Universitaria (5000) Córdoba, Argentina
[2] Facultad de Matemática Astronomía y Física, Universidad Nacional de Córdoba, Medina Allende y Haya de la Torre, Ciudad Universitaria (5000) Córdoba, Argentina

E-mail: carlosdiprinzio@gmail.com, edruetta@gmail.com and onasello@gmail.com

Received 20 July 2012, in final form 5 December 2012
Published 30 January 2013
Online at stacks.iop.org/MSMSE/21/025007

Abstract
Grain growth (GG) processes in the presence of second-phase and stationary particles have been widely studied but the results found are inconsistent. We present new GG simulations in two- and three-dimensional (2D and 3D) polycrystalline samples with second phase stationary particles, using the Monte Carlo technique. Simulations using values of particle concentration greater than 15% and particle radii different from 1 or 3 are performed, thus covering a range of particle radii and concentrations not previously studied. It is shown that only the results for 3D samples follow Zener's law.

1. Introduction

Second-phase and stationary particles inhibit grain growth (GG) and this process is known as Zener pinning or Zener drag. Smith [1] cited for the first time the relationship found by Clarence Zener for the maximum force produced by a single spherical particle at a grain boundary. According to Zener, when the material is polycrystalline and has a volumetric concentration f_v of randomly distributed immobile spherical particles of radius r, the GG process stops when the grain size attains a value R_l given by the following expression:

$$\frac{R_l}{r} = a f_v^b, \tag{1}$$

with $a = 3/4$ and $b = -1$. (According to Wörner *et al* [2], there was a misprint in Smith's original paper and it should be $a = 4/3$).

After Smith [1], very different values for a and b have been reported in the literature [3–19]. However, as Harun *et al* [20] said 'Despite a great deal of progress since then [1], there is still no theory that adequately describes the phenomenon.'

It should be noted that, in the Zener pinning theory, the phenomenon analyzed is three-dimensional (3D) in nature and, as pointed out by Hillert [8], 2D and 3D Zener pinning are completely different phenomena. In fact, Hillert [8] showed that, when a 2D sample is

0965-0393/13/025007+08$33.00

Table 1. Key outcomes of the 2D studies.

	Method	L	a	b	f_v (%)	l
[5]	MC	200	1.7	−0.5	0.5 to 5	1
[7]	TA			−0.5	0.5 to 5	
[8]	TA		1.7	−0.5	<10	
[10]	MC	200	0.6	−0.55	<10	1
						2.7
						4.6
						6.5
						8.6
[11]	MC	500	0.6	−0.52	0.1 to 15	1
						2
						3
[12]	MC	200	1.34	−0.52	0.01 to 10	1
						3
						7
[15]	MC	200	?	−0.5	0.06 to 10	?
[16]	MC	100 to 10 000	1	0.48	0.1 to 10	1

theoretically analyzed following the same assumption as Zener, an equation like (1) is followed but with $a = 1.7$ and $b = -0.5$. Hillert [8] also found that for 3D samples the values of b reported by Smith will be valid only for $f < 0.1$. When $f > 0.1$, the grain boundary particle concentrations will not be random and it will be $a = 1.8$ and $b = -1/3$.

We note that, for all practical purposes, when a theory is needed to predict R_l, the uncertainty in parameter b is of fundamental importance. This becomes crucial when the test sample cannot be subjected to any experimental testing, as in the case of studies carried out to interpret the temporal evolution of grain size observed at different depths in glaciers [21].

Many computer simulation methods have been developed to study the GG phenomenon, including the effect of impurities, anisotropic boundary energies and mobilities and second phase particles, since these effects cannot be resolved analytically within the whole range of possibilities that may be present in real materials. Among these models are the Monte Carlo (MC) [9–15], phase field [16–19], finite element method [22] and cellular automata [23]. Of these, the MC method was the most used because it is the easiest to implement, and also describes many characteristics of the GG process very well, including some aspects of Zener drag [13]. However, still today there are some features of the MC studies that need to be analyzed.

To clarify the current state of the problem, we will make a quick summary of some representative previous studies on Zener drag. We will concentrate on the theoretical analysis (TA) and MC computer simulations carried out in two-dimensional (2D) or 3D samples.

The key outcomes of the different studies in 2D and 3D samples are presented in tables 1 and 2, respectively. These tables specify whether the studies are theoretical or computational, and in the latter case specify the sample sides, L for square or cubic samples, the side of particle l; the range of volumetric concentration f_v and the values of a and b fitting the obtained data with equation (1).

From table 1 the following can be seen.

(1) Theoretical analyses predict b values close to −0.5.
(2) Computer simulations used f_v values between 0.01% and 15%, the results follow the law given by equation (1), with $b = -0.5$ and a values between 0.6 and 1.7 and equation (1) has been checked at different particle sizes.

Table 2. Key outcomes of the 3D studies.

	Method	L	a	b	f_v (%)	l
[1]	TA		0.75	−1	0 to 100	
[8]	TA		0.44	−0.93	<10	
			1.8	−0.33	>10	
[9]	MC	100	4.5	−0.31	0.5 to 5	1
[13]	MC	400	0.72	−1	0.25 to 15	3

Of the works cited in table 1, we also point out the following aspects.

(3) Not all the authors have the same approach to assigning radius to the particles [10–12, 16]: some used $r = l/2$ [12], others $r = (A)^{0.5}/\pi$ with A particle area [5, 16], and others do not specify.
(4) The computer simulations generally showed that the particles have a random distribution. Srolovitz *et al* [5] showed that the fraction of particles at the grain boundaries is almost the same as those in the bulk.
(5) In some cases it can be seen that the particles can touch or overlap. This effect indicates that the corresponding r values must be larger than those of individual particles. Only Hassold *et al* [10] saw that the effect of grouping (clustering) of particles affected the GG.

From table 2 the following can be seen.

(1) According to the theoretical treatment performed by Hillert [8], the value of b in equation (1) may be different for $f_v > 10\%$.
(2) The 3D computer simulations used f_v values between 0.25% and 15% and the results follow the law given by equation (1), with $b = -0.33$ or -1, and $a = 0.2$ or 4.5

Of the works cited in table 2, we also point out the following aspects.

(3) Miodownik *et al* [13] found artificial unpinning for small particle sizes, so they used $r = 3$.
(4) It is known that sample size produces a pinning effect in any GG simulation. In fact, as Miodownik *et al* said [13], when crystals are more than 0.33 times the size of the sample, GG slows due to edge effects, even when the samples are free of particles.

From the literature we can conclude that the b values obtained by different authors with 2D samples are concordant and give a value of $b = -0.5$. However, the values of a are different and the studies performed always use $f_v < 15\%$. On the other hand, the computational results obtained with 3D samples are not consistent and were obtained using only $r = 1$ and 3 and f_v values lower than 15%. Note that according to Hillert [8], the value of b in equation (1) may be different for $f_v > 10\%$, so it is important to investigate the GG using higher values of f_v.

In this work we studied GG in samples with stationary particles, using 2D and 3D MC techniques. We were mainly interested in performing 2D and 3D simulations using f_v values greater than 15% and 3D simulations using particle radii different from 1 or 3, thus covering a range of particle radii and concentrations not previously studied.

2. Method

In this work, we employed an MC algorithm similar to that first used by Anderson *et al* [9]. The algorithm operates on a square matrix of $n \times n \times n$ points, where each site (i, j, k) has an initial orientation $s = j + (i - 1)n + (k - 1)n^2$, where $s \in [0, n^3]$, i.e. the number of different orientations Q is n^3. Particles or precipitates have a cubic shape of side length l and orientations $s = 0$. To generate the particle distribution, a point of the matrix is randomly

selected and then its neighbors are added to obtain a cube particle of volume l^3. The particle-generating algorithm could only study precipitates that have a point at the center, i.e. of side 1, 3, 5, etc. The number of sites with $s = 0$ is called N_0, and the total number of particles is called N_l. Two randomly selected particles could touch or overlap each other if the distance between their centers was less than $2l$. In this case, the size of real particles is higher than l and the average particle size d is calculated by the linear intercept method [24], using only lines parallel to the sides of the samples. The r values in equation (1) were taken as $r = \pi^{-0.5}d$ when 2D samples were analyzed and $r = d(3/4\pi)^{1/3}$ when the samples were 3D.

The MC algorithm was applied as follows.

The effect of temperature T on the exchange between the sites is given by the probability

$$P = \mathrm{e}^{\frac{-\Delta H}{kT}}, \tag{2}$$

where k is the Bolzmann constant and ΔH is the difference in energy. To calculate ΔH, the program took into account the interaction between a site and the first three layers of neighbors (26 neighboring sites). The interaction energy between site n and its neighbors is

$$H_n = \sum_{m=1}^{26} J(1 - \delta_{mn}), \tag{3}$$

where J is a parameter related to the energy between two sites with different orientations and the function δ_{mn} is the Kronecker delta. $J = 0.1kT$ was always used. The program randomly selected a neighbor l of site n, both sites were exchanged in the array and the interaction energy was recalculated, using equation (3). If the change in energy is negative, the change is accepted. If, on the other hand, the energy change is positive, the change is accepted with a probability given by equation (2).

Simulations were performed with particles of initial side $l = 1$, 3 and 5 and fractions of stationary particles in the range from 2% to 70%. 2D samples of $L = 300$ pixel per side and 3D samples of L between 400 and 100 pixels per side were used to avoid the decrease in GG produced by the edge effect of the samples (13, 16). The longest process involved a sample of $L = 400$ pixels per side with a particle concentration $f_\mathrm{v} = 2\%$, and was performed during 300 000 MC steps (MCSs).

3. Results and discussion

The 2D results presented in figure 1 show that the plot $\ln(R_l/r)$ versus $\ln(f_\mathrm{v})$ presents a linear behavior from which the parameters of equation (1) $a = 0.9 \pm 0.1$ and $b = -0.52$ can be extracted. In this figure, it can be seen that the $\ln(R_l/r)$ values corresponding to $l = 1$ are in general slightly larger than those obtained with higher l values. This observation indicates that the temperature fluctuations may have produced an unpinning effect in the 2D samples similar to that observed by [13] in the 3D sample. If the $\ln(R_l/r)$ versus $\ln(f_\mathrm{v})$ the fitting curve is obtained not taking into account the $l = 1$ values, the parameters of equation (1) obtained are $a = 0.9 \pm 0.1$ and $b = -0.482$. These values found using f_v values up to 0.70 and samples of $L = 300$ pixel per side are in complete agreement with those obtained by [16] using f_v values lower than 0.1 and higher values of L. Thus we see that, in 2D, a value of $b = -0.5$ is a good exponent to use in the Zener equation, because theoretical and simulated results are well represented. In consequence, using $b = -0.5$ and fitting again all the $l > 1$ results, we found an $\boldsymbol{a}$ value of $a = 1 \pm 0.1$. It must be noted that this $\boldsymbol{a}$ value is valid for particles of different radii and shape. In fact, in our studies we used particles of $l = 3$ and $l = 5$ and, when the f_v values were high enough to produce particle overlapping, the size of the overlapping particles was greater than the previous ones and their shapes were irregular.

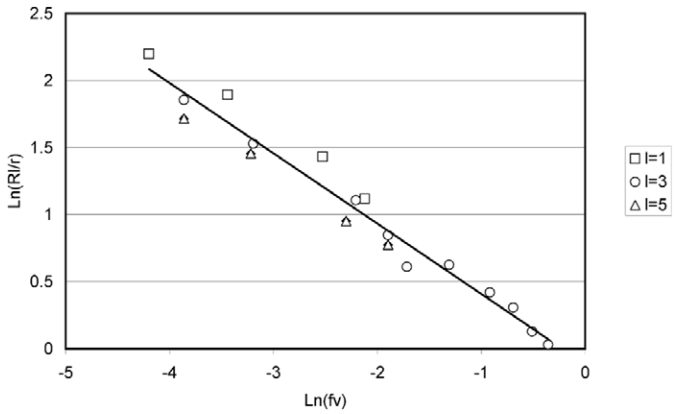

Figure 1. $\mathrm{Ln}(R_l/r)$ versus $\ln(f_v)$ for 2D samples with particle sizes 1, 3 and 5 pixels per side. $r = \pi^{-0.5}d$ with d average particle size calculated by the linear intercept method.

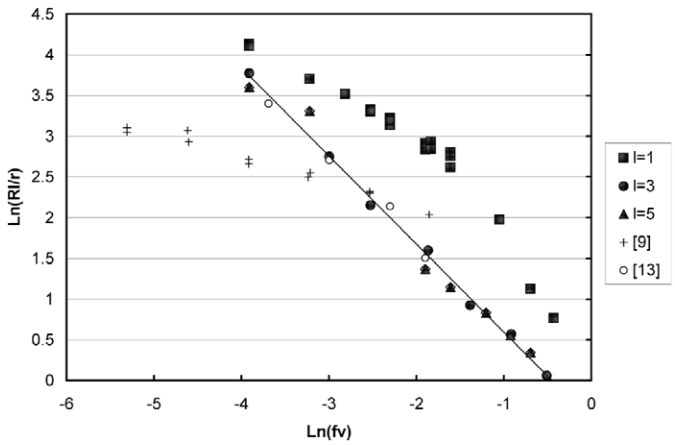

Figure 2. As in figure 2 but for 3D samples. $r = d(3/4\pi)^{1/3}$ with d average particle size calculated by the linear intercept method.

The results obtained in this work and presented by other authors using 3D samples are shown in figure 2. In this figure it can be observed that results obtained with particles of initial size $l = 1$ are different than those obtained with higher l values. With $l = 1$, the final sizes of the grain are in general 1.5 to 2 times higher than those obtained with higher l values. This behavior is similar to the unpinning effect reported by [13]. In figure 2 it can be seen that Anderson *et al*'s $\ln(R_l/r)$ values in general are lower than those obtained in this work, and that the differences between both results increase as f_v decreases. This discrepancy could be caused, as Miodownik *et al* said [13], by an artificial pinning produced by the sample size, and also by the lower temperatures used in these studies. From figure 2 it can also be seen that the plot $\ln(R_l/r)$ versus $\ln(f_v)$, corresponding to the values obtained in this work with particles of initial size $l = 3$ and $l = 5$, presents a linear behavior even for $f_v > 0.15$, matching those reported by [13] for $l = 3$ for $f_v < 0.15$. Miodownik *et al* [13] studied only $f_v < 0.15$, because for higher f_v values, they said that the particles accreted each other, so they were not monodispersed and followed a different behavior.

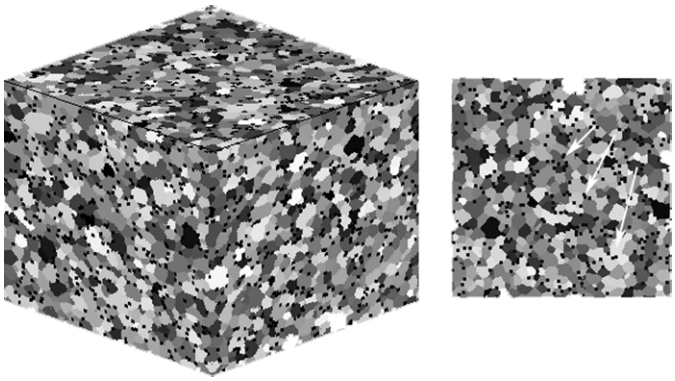

Figure 3. 3D and 2D views of a GG simulation step of polycrystalline sample of 200 pixel by side using $l = 3$ and $f_v = 25\%$.

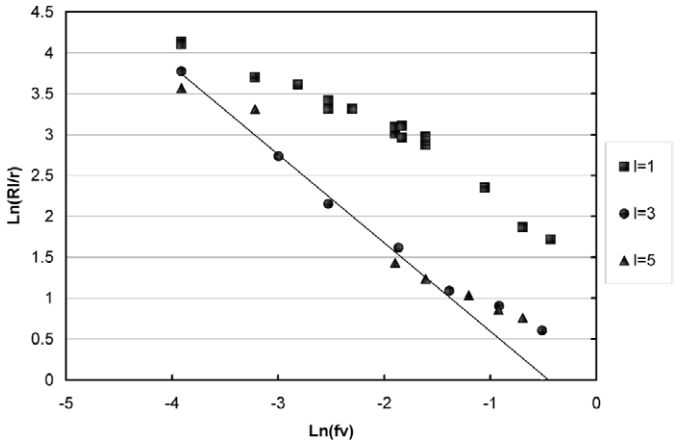

Figure 4. As in figure 2 but using $r = l$. l initial particle size.

In our samples, it may be noted that the particles touched or overlapped (see figure 3). That is, the average size of second phase particles was not the initial particle size. Consequently, if we had not calculated the actual value of the average size of particles using the linear intercept method, the results could be different. The results obtained using the initial particle size $\boldsymbol{l}$ instead of $\boldsymbol{d}$ are shown in figure 4. Comparing figures 2 and 4, we see that using low-concentration values the results are similar, but for high concentrations and $l = 3$ or 5, the slope of the plot $\ln(R_l/r)$ versus $\ln(f_v)$ tends to increase. For particle sizes of side $l = 1$, for high concentrations of particles, the slope of the plot $\ln(R_l/r)$ versus $\ln(f_v)$ also tends to increase, and the total data tend to be linear with a slope of approximately 0.6. Figure 2 shows that, when $l = 1$, the increase in the average real particle size with concentration causes a decrease in R_l/r values, and the values of $\ln(R_l/r)$ tend to be similar to those obtained with higher values of $\boldsymbol{l}$.

Figure 2 also shows that for $\ln(f_v) = -2$ there are various values of $\ln(R_l/r)$, showing a data dispersion of about 30% produced both by the MC method and by the particle size and shape. From the plot of figure 2, corresponding to the values obtained with particles of initial size $l = 3$ and $l = 5$, the parameters of equation (1) $a = 0.7 \pm 0.1$ and $b = -1$ can be extracted. These two values are very close to that found by Zener.

In conclusion, figure 2 shows that, within the scatter normally found in the simulations, the limit size of grains R_l is well-represented by the law given by Zener with $a = 3/4$ and $b = -1$ for the particle radii higher than $l = 1$ and all volume fractions, if the real radius of the particle is used. The results also show that the theoretical values obtained by Hillert for $f_v > 0.1$ are not found in the simulations. This may be explained by the fact that, in the simulations presented in this paper, the particles were found to be randomly distributed, both in volume and in GB, so that Hillert's suppositions for $f_v > 15\%$ are not observed in this study.

4. Summary

In this work we studied the GG with stationary particles in 2D and 3D samples using the Monte Carlo technique. The initial particles were square or cube, of side $l = 1$, 3 and 5 and the particle concentration ranged from 2% to 70%. When two randomly selected particles touch or overlap each other, the size of real particles is higher than l and the average particle size d is calculated by the linear intercept method [24]. To investigate the Zener law, the r values in equation (1) were taken as $r = \pi^{-0.5}d$ when 2D samples were analyzed, and as $r = d(3/4\pi)^{1/3}$ when the samples were 3D.

In 2D samples, the results obtained are quite consistent with those generally found in the literature, i.e. the Zener equation with $b = -0.5$ and $a = 1$ was found to adequately represent the phenomenon, independently of particle size distribution.

In 3D samples, the new simulation performed showed that the limit size of grain R_l obtained with particles of initial size $l = 1$ is different than those obtained with higher l values. In the first case, the final size of the grains is in general 1.5 to 2 times greater than that of those obtained with higher l values. For l values higher than 1 and when the average values of the particle are considered, the limit size of grains R_l is well-represented by Zener's law with $b = -1$. In this case, the value found of $\boldsymbol{a}$ is close to $3/4$ with an uncertainty of about 30% or more, depending on particle distribution and on particle shape. Thus we conclude that the Zener law with $b = -1$ and $a = 3/4$, i.e. not 4/3 as suggested by Wörner *et al* [2], is valid in 3D for all particle sizes (excluding $l = 1$) and all f_v values, while in 2D samples the limit size of the grain is also represented by equation (1) but with $a = 1 \pm 0.1$ and $b = -0.5$.

Acknowledgments

The authors are grateful to José Barcelona for technical support and to SeCyT-UNC and CONICET for financial support.

References

[1] Smith C S 1948 Grains, phases and interfaces: an interpretation of microstructure *Trans. Metall. Soc. AIME* **175** 15–51
[2] Wörner C H and Hazzledine P M 1992 Grain growth stagnation by inclusions or pores *JOM (USA)* **44** 16–20
[3] Sutton P and Balluffi R W 1995 *Interfaces in Crystalline Materials* (Oxford: Elsevier Science Ltd)
[4] Anderson M P, Srolovitz D J, Grest G S and Sahni P S 1984 Computer simulation of grain growth: I. Kinetics *Acta Metall.* **32** 783–91
[5] Srolovitz D J, Anderson M P, Sahni P S and Grest G S 1984 Computer simulation of grain growth: II. Grain size distribution, topology, and local dynamics *Acta Metall.* **32** 793–802
[6] Srolovitz D J, Anderson M P, Grest G S and Sahni P S 1984 Computer simulation of grain growth: III. Influence of a particle dispersion *Acta Metall.* **32** 1429–38

[7] Doherty R D, Srolovitz D J, Rollett A D and Anderson M P 1987 On the volume fraction dependence of particle-limited grain growth *Scr. Metall.* **21** 675–79
[8] Hillert M 1988 Inhibition of grain growth by second-phase particles *Acta Metall.* **36** 3177
[9] Anderson M P, Grest G S, Doherty R D, Li K and Srolovitz D J 1989 Inhibition of grain growth by second phase particles: three dimensional Monte Carlo computer simulation *Scr. Metall.* **23** 753–8
[10] Hassold G N, Holm E A and Srolovitz D J 1990 Effects of particle size on inhibited grain growth *Scr. Metall. Mater.* **24** 101–6
[11] Gao J, Thompson R G and Patterson B R 1997 Computer simulation of grain growth with second phase particle pinning *Acta Mater.* **45** 3653–58
[12] Soucail M, Messina R, Cosnuau A and Kubin L P 1999 Monte Carlo simulation of Zener pinning in two dimensions *Mater. Sci. Eng.* A **271** 1–7
[13] Miodownik M A, Holm E A and Hassold G 2000 Highly parallel computer simulations of particle pinning: zener vindicated *Scr. Mater.* **42** 1173–77
[14] Miodownik M A, Martin J W and Cerezo A 1999 Mesoscale simulations of particle pinning *Phil. Mag.* A **79** 203–22
[15] Ming Huang C, Joanne C L, Patnaik B S V and Jayaganthan R 2006 Monte Carlo simulation of grain growth in polycrystalline materials *Appl. Surf. Sci.* **252** 3997–4002
[16] Phaneesh K R, Bhat A, Mukherjee P and Kashyap K T 2012 On the Zener limit of grain growth through 2D Monte Carlo simulation *Comput. Mater. Sci.* **58** 188–191
[17] Moelans N, Blanpain B and Wollants P 2006 Phase field simulation of grain growth in three dimensional system containing finely dispersed second-phase particles *Acta Mater.* **54** 1175–84
[18] Moelans N, Blanpain B and Wollants P 2007 Pinning effect of second-phase particles on grain growth in polycrystalline films studied by 3-D phase field simulations *Acta Mater.* **55** 2173–82
[19] Suwa Y, Saito Y and Onodera H 2006 Phase field simulation of grain growth in three dimensional system containing finely dispersed second-phase particles *Scr. Metall.* **55** 407–10
[20] Harun A, Holm E A, Clode M P and Miodownik M A 2006 On computer simulation methods to model Zener pinning *Acta Mater.* **54** 3261–73
[21] Alley R 1992 Flow-law hypotheses for ice-sheet modeling *J. Glaciol.* **38** 245–56
[22] Uyar F, Wilson S R, Gruber J, Lee S, Sintay S, Rollett A D and Srolovitz D J 2009 Testing a curvature driven moving finite element grain growth model with the generalized three dimensional von Neumann relation *Int. J. Mater. Res.* **100** 543–9
[23] Lan Y, Li D and Li Y 2006 A mesoscale cellular automaton model for curvature-driven grain growth *Metall. Mater. Trans.* B **37** 119–29
[24] Han J H and Kim D Y 1998 Determination of three-dimensional grain size distribution by linear intercept measurement *Acta Mater.* **46** 2021–28